



Study of structural changes in amorphous germanium–nitrogen alloys by optical techniques

A. R. Zanatta, I. Chambouleyron, and P. V. Santos

Citation: *Journal of Applied Physics* **79**, 433 (1996); doi: 10.1063/1.360849

View online: <http://dx.doi.org/10.1063/1.360849>

View Table of Contents: <http://scitation.aip.org/content/aip/journal/jap/79/1?ver=pdfcov>

Published by the [AIP Publishing](#)

Articles you may be interested in

[Optical diffraction gratings produced by laser interference structuring of amorphous germanium–nitrogen alloys](#)
Appl. Phys. Lett. **81**, 2731 (2002); 10.1063/1.1512307

[Thermomechanical properties of amorphous hydrogenated germaniumnitrogen alloys](#)
AIP Conf. Proc. **378**, 315 (1996); 10.1063/1.51222

[Valence band structure of amorphous germaniumnitrogen alloys](#)
AIP Conf. Proc. **378**, 310 (1996); 10.1063/1.51112

[Bandgap tailoring in amorphous hydrogenated germaniumnitrogen alloys](#)
AIP Conf. Proc. **378**, 300 (1996); 10.1063/1.51110

[Study of amorphous germaniumnitrogen alloys through xray photoelectron and Auger electron spectroscopies](#)
Appl. Phys. Lett. **66**, 1258 (1995); 10.1063/1.113255



AIP | Journal of Applied Physics

Journal of Applied Physics is pleased to announce **André Anders** as its new Editor-in-Chief

Study of structural changes in amorphous germanium–nitrogen alloys by optical techniques

A. R. Zanatta and I. Chambouleyron^{a)}

Instituto de Física “Gleb Wataghin,” UNICAMP, 13083-970 Campinas, São Paulo, Brazil

P. V. Santos

Max-Planck-Institute für Festkörperforschung, D-70569 Stuttgart, Germany

(Received 23 June 1995; accepted for publication 11 September 1995)

Thin films of amorphous germanium–nitrogen (*a*-GeN) alloys prepared by the rf sputtering deposition technique have been studied by Raman scattering spectroscopy. The nitrogen content of the samples varies between zero and $\approx 3 \times 10^{22}$ atoms cm^{-3} , as determined from nuclear reaction analysis data. Modifications of the structural characteristics of the Ge–N alloys, probed through their phonon density, were investigated as a function of the nitrogen concentration. In addition to an increase of the network's topological disorder, nitrogen is responsible, at relatively high concentrations, for a structural transition in the *a*-Ge host. The optical and electronic characterization of the samples confirm these changes which are highly dependent on the nitrogen concentration. © 1996 American Institute of Physics.[S0021-8979(96)01001-9]

I. INTRODUCTION

The optoelectronic properties of crystalline (*c*-) and amorphous (*a*-) semiconductors are sensitive to small changes, intentional or not, of their structure. Some optoelectronic characteristics can be tailored by intentional chemical doping and/or by alloying different elements. In fact, many semiconductor applications are the mere result of a judicious use of these “perturbations.” As a consequence, structural studies of semiconducting alloys are nowadays one of the main concerns of semiconductor science and technology. Infrared (IR) and Raman scattering spectroscopies are well-developed probe techniques. The analysis of lattice or network vibration modes has proved to be an efficient tool in structural studies.

Subject to the applicable selection rules, first-order IR absorption occurs when the frequency of the incident radiation matches the characteristic frequency of the absorbing vibration mode. In a Raman, or inelastic, light-scattering process, the incident light (usually a laser source) is frequency shifted by an amount equal to the natural frequency of the vibration mode. The optical investigation of network vibrations in *a*-semiconductors is favored by the fact that the absence of long-range order (LRO) makes possible the observation of all those vibration modes whose detection in crystalline materials is usually forbidden by selection rules.

Since the short-range order (SRO) in *a*-semiconductors is similar to that in the crystalline parents, the phonon density of states is expected to be similar to that of the crystalline phase with some broadening due to the inherent disorder in bond length and angle. In addition to structural information, Raman scattering measurements in *a*-semiconductors can give insight into the bond type and the nature of disorder. As a result, Raman studies provide valuable dynamical and structural information of *a*-semiconductors, as well as on their dependence on preparation conditions and/or composition.^{1,2}

In this work we present a Raman scattering study of *a*-GeN alloys. Emphasis is given to the structural changes produced by different nitrogen concentrations in the *a*-Ge network. Raman results are compared with those obtained from other optical and electronic characterizations, as well as with calculations. The present article corroborates the expected change of the bonding character of these alloys, from predominantly *sp*³-like (essentially Ge–Ge bonds) to some combination of *sp*³- and *sp*²- (or *p*-) like orbitals associated with Ge–Ge and Ge–N bonds, respectively.

II. EXPERIMENTAL DETAILS

The *a*-Ge and *a*-GeN samples were prepared by rf sputtering a pure *c*-Ge target in an Ar+(N₂) atmosphere. The N₂ partial pressure was adjusted before each deposition run and kept constant during the growth process. With the exception of the N₂ partial pressure (see Table I) all the other deposition parameters were the same for all samples.³ Polished intrinsic *c*-Si wafers were used as substrates for IR and Raman measurements. Optical absorption in the near-infrared (NIR) and visible (VIS) energy ranges and photothermal deflection spectroscopy (PDS) measurements were performed on films codeposited on Corning 7059 glass substrates. From the optical-absorption measurements⁴ (in the 0.6–3.5 eV photon energy range) the optical-gap-related parameters E_{04} and E_{Tauc} and Tauc's $B^{1/2}$ parameter were determined. From the analysis⁵ of the PDS data (in the 0.5–2.5 eV range) the characteristic energy E_0 of the exponential (Urbach) absorption edge was obtained.

The nitrogen content of the *a*-GeN alloys was determined from a deuteron-induced nuclear reaction [¹⁴N(*d*,*p*)¹⁵N]. The method allows the determination of nitrogen contents as low as $[N] \approx 10^{19}$ atoms cm^{-3} in samples having a typical thickness of 10^{-4} cm (see Table I). The analysis was done in a 4 MeV van de Graaff accelerator, with an incident deuterium beam of 610 keV. Detailed information on the deposition conditions and on the optoelectronic

^{a)}Electronic mail: ivanch@ccvax.unicamp.br

TABLE I. Main characteristics of the *a*-GeN sample series. P_{N_2} and d are the nitrogen partial pressure during deposition and the film thickness, respectively. $[N]_{\text{NRA}}$ represents the nitrogen content in the samples as determined from nuclear reaction analysis, E_{04} is the energy corresponding to an absorption coefficient of 10^4 cm^{-1} , and E_0 is the characteristic Urbach edge (as determined from PDS measurements). Note: b and na mean below the detection limit and not available, respectively.

Sample no.	P_{N_2} (mbar)	d (μm)	$[N]_{\text{NRA}}$ (atoms cm^{-3})	E_{04} (eV)	E_0 (meV)
1	$<10^{-7}$	1.15	b	0.84	135
2	5.0×10^{-6}	1.04	na	0.86	140
3	8.6×10^{-6}	1.00	na	0.85	147
4	1.5×10^{-5}	1.13	1.6×10^{20}	0.84	137
5	4.0×10^{-5}	1.00	6.0×10^{20}	0.86	150
6	7.0×10^{-5}	1.03	9.1×10^{20}	0.83	155
7	2.4×10^{-4}	1.04	3.0×10^{21}	0.84	162
8	7.5×10^{-4}	1.08	8.8×10^{21}	0.90	165
9	2.2×10^{-3}	1.04	1.8×10^{22}	1.16	219
10	7.5×10^{-3}	1.02	2.5×10^{22}	2.25	261
11	1.5×10^{-2}	0.65	2.9×10^{22}	2.48	222

properties of the present *a*-GeN samples can be found in Ref. 3.

The Raman spectra were recorded on a multichannel Raman setup using an excitation wavelength of 476.5 nm from an Ar^+ laser. In order to reduce the elastic scattered light close to the laser line the measurements were performed with crossed incident and scattered polarization (the independence of the line shape of the Raman spectra on the scattering geometry has been checked). All measurements were performed in air and at room temperature.

Table I indicates the nitrogen partial pressure P_{N_2} employed during deposition, the film thickness and its nitrogen content, as well as the optical characteristics of the studied *a*-GeN samples. Note that sample no. 1 corresponds to a nitrogen-free amorphous germanium film.

III. EXPERIMENTAL RESULTS

A. Optical-absorption spectroscopy

Amorphous semiconductors do not have a well-defined optical gap. As a consequence, it is common practice to consider E_{04} (the photon energy corresponding to an absorption coefficient $\alpha = 10^4 \text{ cm}^{-1}$) as a measure of the absorption edge energy. Another definition is the so called Tauc's gap E_{Tauc} which is given by the energy where the $(\alpha n E)^{1/2}$ or $(\alpha E)^{1/2}$ vs E plot, where n is the index of refraction and E the photon energy, goes to zero. According to this definition,

$$(\alpha E)^{1/2} = B^{1/2}(E - E_{\text{Tauc}}), \quad (1)$$

the slope $B^{1/2}$ (or Tauc's $B^{1/2}$ parameter) is associated with the steepness or tailing degree of the joint density of states (DOS) near the band edges ($\alpha \geq 10^4 \text{ cm}^{-1}$). Figure 1 shows the measured E_{04} and E_{Tauc} , and the Tauc's $B^{1/2}$ parameter, as a function of the nitrogen content in the present *a*-GeN alloy series as determined from the optical-absorption data. The band gap and the slope parameter $B^{1/2}$ remain approximately constant up to a nitrogen content of around 10^{22} atoms cm^{-3} . For nitrogen contents higher than this value, a rather abrupt change is measured in the optical parameters in a way similar to that reported for *a*-SiN alloys.⁶

With increasing amorphicity, the sharp absorption edge characteristic of crystals broadens into tails of localized states extending into the pseudogap. These localized states arise from weak bonds, which in turn originate from deviations from ideal bond length and bond angle, a characteristic of topological disorder. The energy distribution of tail states is associated with the Urbach energy E_0 , or the characteristic energy of the exponential absorption edge, i.e.,

$$\alpha = \alpha_0 \exp(-E/E_0). \quad (2)$$

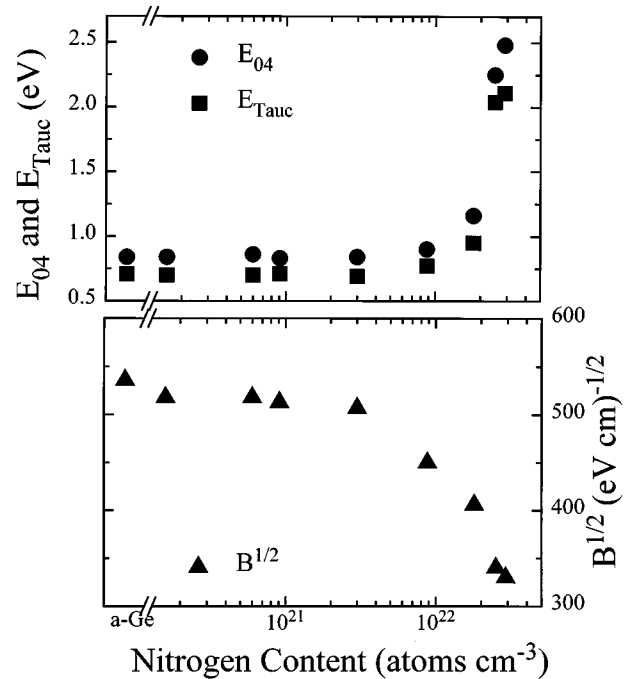


FIG. 1. Tauc's $B^{1/2}$ parameter and optical gaps E_{04} and E_{Tauc} as a function of the nitrogen content. It can be clearly seen that both E_{04} and E_{Tauc} present an abrupt increase at $[N] \geq 10^{22}$ atoms cm^{-3} . Note that the Tauc's $B^{1/2}$ parameter appears to be more sensitive to N content than the optical gap, a consequence of the changes of the character of the electronic states at the VBM.

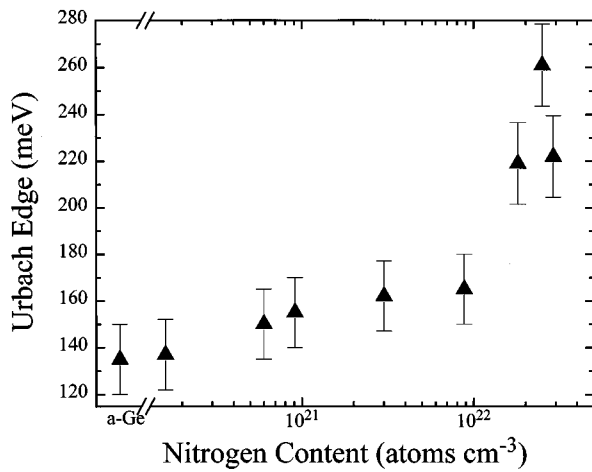


FIG. 2. Urbach edge characteristic energy (as determined from PDS measurements) as a function of the nitrogen content in *a*-GeN alloys. As shown in the figure, two different regimes can be identified, according to the nitrogen concentration in the samples. In the Ge-rich regime ($[N]$ up to $\approx 10^{22}$ atoms cm^{-3}) the presence of nitrogen atoms is responsible for a steady increase of the topological disorder. Nitrogen concentrations higher than 10^{22} atoms cm^{-3} are responsible for abrupt structural changes.

The exponential absorption edge region usually covers the $10 \text{ cm}^{-1} \leq \alpha \leq 10^4 \text{ cm}^{-1}$ range, and roughly represents the distribution of the valence-band (VB) tail states, which is broader than the conduction-band (CB) tail. The characteristic energy of the Urbach edge of *a*-GeN samples as a function of nitrogen content is shown in Fig. 2.

B. Raman scattering

Figure 3 shows the Raman spectra of some *a*-GeN samples with increasing nitrogen concentration. In the case of pure *a*-Ge, the spectrum measured at room temperature is dominated by the contributions from the TA-like mode at $\approx 80 \text{ cm}^{-1}$ (the apparent frequency shift of this mode is due to monochromator filtering effects below $\approx 100 \text{ cm}^{-1}$) and

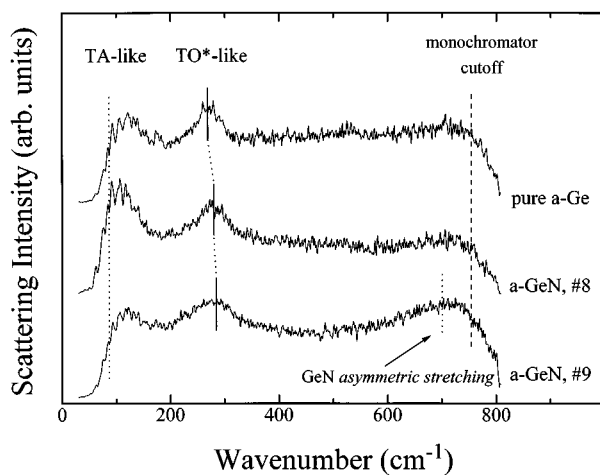


FIG. 3. Reduced Raman spectra of some *a*-Ge(N) samples with increasing nitrogen concentrations. The energies corresponding to the TA- ($\approx 80 \text{ cm}^{-1}$) and TO*-like ($\approx 270 \text{ cm}^{-1}$) vibration modes, as well as the GeN in-plane asymmetric stretching vibration mode ($\approx 700 \text{ cm}^{-1}$), are also indicated.

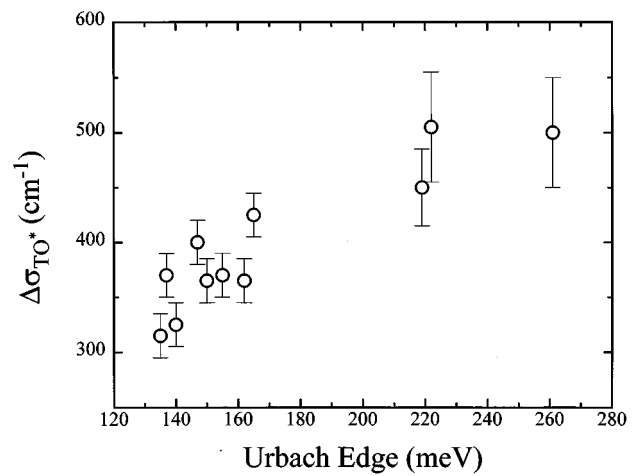


FIG. 4. Full width at half-maximum height [FWHM ($\Delta\sigma_{\text{TO}^*}$)] of the TO*-like mode as a function of the Urbach edge characteristic energy E_0 . A clear relationship between the two indicators of topological disorder is apparent from the figure.

from the TO*-like mode at $\approx 270 \text{ cm}^{-1}$. A nitrogen content of up to $\approx 10^{22}$ atoms cm^{-3} does not affect significantly the spectral shape, except for a slight broadening of the TO*-like mode. For larger nitrogen concentrations, however, radical changes are observed. The TA- and TO*-like modes broaden considerably and are also shifted to higher energies. In addition, a broad structure appears at $\approx 700 \text{ cm}^{-1}$ corresponding to the in-plane asymmetric stretching vibration mode of the N-Ge₃ skeleton, identified from IR transmission data.³ For all samples, the average frequency (ω_{TO^*}), the intensity (I_{TO^*}), and the full width at half-maximum height FWHM ($\Delta\sigma_{\text{TO}^*}$) of the TO*-like mode, were determined from the reduced Raman spectra.² Figure 4 shows $\Delta\sigma_{\text{TO}^*}$ as a function of the Urbach edge energy for the whole sample series. Figure 5 displays the measured Raman peak energy of the Ge-Ge TO*-like mode and the wave number of the IR peak

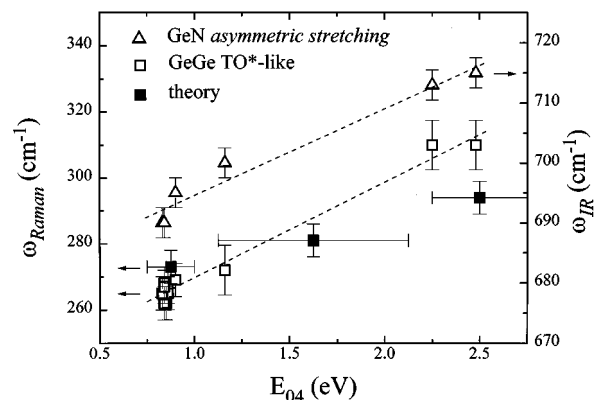


FIG. 5. Frequency shifts of the Ge-N in-plane asymmetric stretching ω_{IR} and of the TO*-like (ω_{TO^*}) vibration modes as a function of the optical parameter E_{04} (which depends on nitrogen concentration). Both the asymmetric stretching vibration and TO*-like modes display a similar behavior. Also represented are theoretical data from Barrio *et al.* (Ref. 21) showing the expected increase of the TO*-like mode frequency. Large nitrogen contents are responsible for a lightening and a stiffening of the network. The dashed straight lines are linear regression fits of experimental data.

of the in-plane asymmetric stretching vibration of the N–Ge₃ skeleton, as a function of the optical parameter E_{04} .

IV. DISCUSSION

A. Optical-absorption spectroscopy

Figures 1 and 2 indicate that for $[N] < 10^{22}$ atoms cm^{-3} (Ge-rich alloys), E_{04} and the Urbach energy (associated to the degree of disorder) increase slowly with nitrogen content. An increased topological disorder is expected on alloying, since nitrogen and germanium have quite different size and electronic configurations. Nitrogen contents $[N] \geq 10^{22}$ atoms cm^{-3} (alloy phase), on the other hand, induce a rather abrupt change of the optical gap (see Table I and Fig. 1), as well as a drastic reduction of the conductivity.^{3,6} A marked decrease of $B^{1/2}$ also occurs for $[N] \geq 10^{22}$ atoms cm^{-3} , the nitrogen content at which the material experiences structural modifications.³ The abrupt changes of both $B^{1/2}$ and the optical gap originate from a change of the bonding character and of the electronic states at the valence-band maximum (VBM), as corroborated from ultraviolet photoemission spectra (UPS).⁷ The UPS experimental data indicate a decreasing contribution of the Ge 4*p* orbital to the VB maximum. The concomitant appearance of N 2*p* (nonbonding) orbitals is detected. As long as the Ge 4*p* orbitals dominate the top of the VB no significant changes of E_{04} are measured. The influence of N 2*p* orbitals is found to be dominant for $[N] > 10^{22}$ atoms cm^{-3} . Thus, the change of the electronic states dominating the VB maximum is the main reason for the abrupt opening of the band gap (see Fig. 1). The situation being depicted is similar to the case of *a*-SiN alloys.⁸

B. Raman scattering

The vibration density of states of *c*-semiconductors possesses four dominant structures in cubic lattices:

- (1) the TA peak, due to zone-edge transverse acoustic phonons at the *L*, *X*, and *K* points of the Brillouin zone;
- (2) the LA peak, due to longitudinal acoustic phonons at the *L* point;
- (3) the LO peak, due to longitudinal optic phonons at *L* and *K* points; and
- (4) the TO peak, caused by the transverse optic phonons at *X* and *L* points.¹

The overall shape of the vibration density of states of *a*-semiconductors can be qualitatively related to the crystalline density of vibration states by convoluting it with a suitable broadening function, a consequence of the inherent topological disorder.⁹ It should not be surprising that the amorphous spectrum is a broadened version of the crystalline parent, since the vibration modes are mainly determined by bond-length and bond-angle force constants and these reflect the local (or short-range) order (SRO) which is almost the same in both cases. As a consequence, it is common practice to label the various vibration bands in the Raman spectrum of *a*-semiconductors using the crystalline denominations, TA, LA, LO, and TO. In the Raman spectra of *a*-semiconductors, the TA- and TO-like modes have intensities higher than the LA- and LO-like modes. Considering the

closeness and, in some cases, the overlapping of the vibration modes of *a*-semiconductors, we designated the TO- as TO*-like mode, including in this way the probable contributions (mainly in the low-frequency tail) of the LA- and LO-like vibration modes.

Raman scattering studies on *a*-semiconductors have shown that a correspondence exists between the deposition conditions of the films and the measured spectra.^{10–13} Similar investigations have been performed in order to determine the influence of impurities in the spectra of *a*-semiconductor hosts.^{13–16} There is wide agreement on the fact that the FWHM of the TO-like vibration mode $\Delta\sigma_{\text{TO}}$ and the $I_{\text{TA}}/I_{\text{TO}}$ ratio are useful indicators of structural disorder, a larger disorder corresponding to larger FWHM and $I_{\text{TA}}/I_{\text{TO}}$ values. Roughly speaking, changes in $\Delta\sigma_{\text{TO}}$ correspond to modifications in the SRO, particularly in the bond-angle distribution. The $I_{\text{TA}}/I_{\text{TO}}$ ratio changes are primarily due to modifications of the TO-like mode, which diminishes in intensity as a result of broadening. The relative constancy of the TA-like contribution is consistent with theoretical density-of-states calculations which indicate rather small changes in the TA-like intensity up to relatively large bond-angle disorder values.^{17,18} It is important to note that this mode is sensitive just to the intermediate-range order (IRO). The broadening of the TO*-like mode and its shift to lower phonon frequencies have been used to measure the degree of disorder in *a*-semiconductors.¹⁹

The laser energy (2.6 eV) used to record the Raman spectra (Fig. 3) is expected to couple mainly the valence and conduction states associated with the Ge–Ge bonds. The corresponding states of the Ge–N bonds have a higher-energy separation, as is attested by the large band gap of the nitrogen-rich samples: These states resonate weakly with the incident laser field. As a result, the changes in frequency and linewidth of the TO*-like mode in Fig. 3 basically reflect the distortion of the Ge–Ge bonds with increasing N concentration. Figure 4 shows the FWHM of the TO*-like mode ($\Delta\sigma_{\text{TO}^*}$) as a function of the Urbach edge E_0 . As expected, $\Delta\sigma_{\text{TO}^*}$ increases with E_0 since both parameters are associated with distorted bonds, i.e., larger E_0 values corresponding to greater topological disorder. As a consequence of the high sensitivity of $\Delta\sigma_{\text{TO}^*}$ to the SRO, the changes become more important at nitrogen contents higher than 10^{22} atoms cm^{-3} , or in the N-rich regime. For small nitrogen contents, $[N] \leq 10^{22}$ atoms cm^{-3} , the symmetry of the bonds is mostly determined by the sp^3 -like character of the Ge–Ge bonds. The changes measured for large nitrogen content (N-rich samples) are attributed to the drastic bond-angle distortions due to changes in the character of the dominating bonds of the network, from essentially sp^3 -like (Ge–Ge) to some combination between sp^3 - and sp^2 - (or *p*-) like orbitals (Ge–N).²⁰

Figure 5 displays the in-plane asymmetric stretching frequencies ω_{IR} of the N–Ge₃ skeleton as determined from IR analyses,³ and the TO*-like Raman frequency shift ω_{Raman} as a function of the optical parameter E_{04} (which in turn depends on the nitrogen content, see Fig. 1 and Table I). Figure 5 also shows the expected shifts with increasing nitrogen content from a vibration DOS calculation based on a simple

effective-medium theory.²¹ According to the figure a remarkable frequency increase of both the Ge–N asymmetric stretching and TO*-like vibration modes is measured as the nitrogen content (or optical gap) increases. The experimental shifts, however, are larger than those predicted by the calculations of Ref. 21.

The IR vibration and Raman scattering frequency shifts shown in Fig. 5 can be understood on the basis of a lightening and a stiffening of the network. Roughly, ω_{Raman} and ω_{IR} are proportional to $(k/\mu)^{1/2}$, where k is an effective force constant associated with the Ge–Ge and the Ge–N bonds, respectively, and μ is the correspondent reduced mass. As nitrogen is added to the *a*-Ge host, heavy Ge atoms are substituted by light N. In addition, Ge–N bonds are stronger than Ge–Ge bonds ($E_B^{\text{GeN}} \approx 2.65$ eV and $E_B^{\text{GeGe}} \approx 1.94$ eV),²² producing a stiffening of the network.

IR transmission spectra of these alloys give support to these considerations.³ Inductive effects in Ge–N dipoles, due to increasing nitrogenation, have been measured in the main in-plane asymmetric stretching vibration mode. They induce a 25 cm⁻¹ shift (from 690 to 715 cm⁻¹, see Fig. 5). In addition, new IR-absorption bands at ≈ 870 and ≈ 1100 cm⁻¹ appear due to back-bonded nitrogen atoms in the neighborhood of the Ge–N dipole.³ All the inductive effects measured in IR transmission spectra derive from a charge-transfer mechanism between Ge and N atoms. X-ray photoelectron spectroscopy (XPS) measurements, performed on the samples under consideration, corroborate the expected charge transfer from Ge to N atoms.^{23,24} The IR transmission study also allows the detection of an absorption band at around ≈ 300 cm⁻¹ due to Ge–Ge dipoles. This absorption band was identified as a disorder-induced breathing vibration mode which becomes IR active as a consequence of deformations in the Ge–Ge bonds produced by charge transfer in their vicinity.³ The off-plane vibrations of the N atom in the N–Ge₃ skeleton, which should occur at ~ 400 cm⁻¹, are detected in IR spectra at high N content,³ but being Raman inactive it does not appear in Fig. 3.

Figures 1, 2, and 4, as well as the whole discussion in the text, strongly support the assumption that (at least in the N-rich regime) disorder increases due to modifications of the character of the dominating bond in the network. The behavior of $\Delta\sigma_{\text{TO}^*}$ with [N] suggests that, besides the expected increase of bond-angle distortion, some changes in the intermediate range order are also taking place. This because the structure evolves from bond angles of $\approx 109^\circ$ (*sp*³-like configuration) to a mixture of angles at $\approx 109^\circ$ and $\approx 120^\circ$ (*sp*²-like configuration).²⁵ It must be stressed that the observed changes in $\Delta\sigma_{\text{TO}^*}$ are not due to changes occurring in the bonding units, but just to the bond-angle distribution. It is also convenient at this point to emphasize the great difference between *a*-GeN and *a*-Si:H (the prototype for *a*-semiconductor studies). In the latter, a crude picture of the bonding configuration suffices to give a fair description of the hydrogen alloyed material, owing to the extremely small mass of H and to its unity coordination. On the other hand, N has a higher coordination number (three or four) and can considerably distort the germanium network. The N-related modes in *a*-GeN represent true bands totally coupled to the

a-Ge network, invalidating the local picture which is essentially useful in *a*-Si:H. As a consequence charge transfer, as well as mass and force constant coupling must be considered carefully. These differences have been discussed in Ref. 21.

V. CONCLUSIONS

The main conclusions of the work follow.

(i) Nitrogen concentrations up to $\approx 10^{22}$ atoms cm⁻³ in the *a*-Ge network provoke a significant increase of the inherent topological disorder, mainly due to bond-angle variations. The augmented disorder has been clearly established by Raman spectroscopy and optical-absorption (PDS) measurements;

(ii) A nitrogen content higher than $\approx 10^{22}$ atoms cm⁻³ induces important changes in the *a*-Ge host tetrahedral bonding units. The N-induced changes of the bonding character of the host network have been studied and corroborated with Raman, IR, optical, and photoelectron spectroscopies. They suggest an overall alloy bonding picture analogous to *a*-SiN alloys;

(iii) A transition from predominantly *sp*³-like to some combination of *sp*³- and *sp*²- (or *p*-) like of the bond character results in:

- (a) changes in the atomic bond-angle distribution (for the whole studied [N] range, $0 \leq [N] \leq 3 \times 10^{22}$ atoms cm⁻³, $\Delta\sigma_{\text{TO}^*}$ increases with N content), and
- (b) a lightening and a stiffening of the amorphous network as the nitrogen content increases in the alloy as suggested by the behavior of both the in-plane asymmetric stretching vibration mode and the TO-like mode (ω_{TO^*}).

ACKNOWLEDGMENTS

The authors are indebted to Professor F. L. Freire, Jr. (PUC-RJ) and to Dr. C. F. O. Graeff (WSI-München) for the NRA and PDS measurements, respectively. This work was partially supported by the Brazilian agencies FAPESP and CNPq.

¹J. S. Lannin, in *Semiconductors and Semimetals* (Academic, New York, 1984), Vol. 21, Part B, Chap. 6, and references therein.

²M. H. Brodsky, in *Light Scattering in Solids I*, Topics in Applied Physics, Vol. 8, edited by M. Cardona (Springer, Berlin, 1983), Chap. 5, and references therein.

³A. R. Zanatta and I. Chambouleyron, Phys. Rev. B **48**, 4560 (1993).

⁴R. Swanepoel, J. Phys. E **16**, 1214 (1983).

⁵H. Curtins and M. Frave, in *Amorphous Silicon and Related Materials*, edited by H. Fritzsche (World Scientific, Singapore, 1988), Vol. A, p. 329.

⁶For *a*-SiN alloys, see, for example, J. Robertson, Philos. Mag. B **69**, 307 (1994).

⁷D. Comedi, A. R. Zanatta, F. Alvarez, and I. Chambouleyron, J. Non-Cryst. Solids (to be published).

⁸R. Karcher, L. Ley, and R. L. Johnson, Phys. Rev. B **30**, 1896 (1984).

⁹J. E. Smith, Jr., M. H. Brodsky, B. L. Crowder, M. I. Nathan, and A. Pinczuk, Phys. Rev. Lett. **26**, 642 (1971).

¹⁰J. S. Lannin, L. J. Piliore, S. T. Kshirsagar, R. Messier, and R. C. Ross, Phys. Rev. B **26**, 3506 (1982).

¹¹L. J. Piliore, N. Maley, N. Lustig, and J. S. Lannin, J. Vac. Sci. Technol. A **1**, 388 (1983).

¹²J. E. Yehoda and J. L. Lannin, J. Vac. Sci. Technol. A **1**, 392 (1983).

¹³N. Maley, J. S. Lannin, and B. A. Scott, J. Non-Cryst. Solids **59&60**, 201 (1983).

- ¹⁴A. Morimoto, S. Oozora, M. Kumeda, and T. Shimizu, *Solid State Commun.* **47**, 773 (1983).
- ¹⁵T. Shimizu, *J. Non-Cryst. Solids* **59&60**, 117 (1983).
- ¹⁶M. B. Tzolov, N. V. Tzenov, and D. I. D. Malinowska, *J. Appl. Phys.* **74**, 2731 (1993).
- ¹⁷D. Beeman and B. L. Bobbs, *Phys. Rev. B* **12**, 1399 (1975).
- ¹⁸P. E. Meek, in *The Physics of Non-Crystalline Solids*, edited by G. H. Frischat (Trans. Tech., Zürich, 1977), p. 586.
- ¹⁹R. A. Street, *Hydrogenated Amorphous Silicon* (Cambridge University Press, Cambridge, 1991).
- ²⁰The phenacite structure of β -Ge₃N₄ with planar N and tetrahedral bonded Ge atoms is consistent with sp^3 Ge hybrid orbitals while N bonding can be explained in terms of a linear combination of p orbitals, the planar geometry being a result of the strong repulsion of nonbonded Ge atoms.
- The VB results from nonbonding N p_z^2 electrons. An alternative bonding configuration could be a N sp^2 hybridization associated with a N p_z^2 nonbonding orbital, resulting in a hcp structure.
- ²¹R. A. Barrio, A. S. Carriço, F. C. Marques, J. Sanjurjo, and I. Chambouleyron, *J. Phys. Condens. Matter* **1**, 69 (1989).
- ²²F. A. Cotton, G. Wilkinson, and P. G. Gaus, *Basic Inorganic Chemistry* (Wiley, New York, 1987).
- ²³A. R. Zanatta, R. Landers, S. G. C. de Castro, G. G. Kleiman, I. Chambouleyron, and M. L. Grilli, *Appl. Phys. Lett.* **66**, 1258 (1995).
- ²⁴A. R. Zanatta and I. Chambouleyron, *Solid State Commun.* **95**, 207 (1995).
- ²⁵See, for instance, F. Yndurain and P. Ordejon, *Philos. Mag. B* **70**, 535 (1994), and references therein.